IJFANS INTERNATIONAL JOURNAL OF FOOD AND NUTRITIONAL SCIENCES
ISSN PRINT 2319 1775 Online 2320 7876
 UGC CARE Listed (Group -I) Journal Volume 11, Iss 01, 2022

A CUCKER–SMALE MODEL WITH NOISE AND DELAY

Dr. M Kothandaraman, Dr. K.Raghunath, G.Madhusudhana

[1,2]professor, [3]Assistant Professor

Department of Maths

Bheema Institute of Technology and Science, Adoni

Abstract:

The Cucker-Smale model for collective animal behavior is studied as a generalization. A system of delayed stochastic differential equations is used to formulate the model. It includes two other processes that are present in animal decision making but are sometimes overlooked in modeling: (i) individual behavior stochasticity, or flaws, and (ii) individual delayed responses to environmental cues. Using an appropriate Lyapunov functional, sufficient conditions for flocking for the generalized Cucker-Smale model are given. As a byproduct, one obtains a novel result concerning the delayed geometric Brownian motion's asymptotic nature. The paper's second section presents the findings from systematic numerical simulations. They not only show the analytical conclusions, but they also allude to a behavior of the system that is a little surprising—namely, that flocking might be made easier by adding an intermediate time delay.

Key words: geometric Brownian motion, noise, delay, flocking, asymptotic behavior, and ucker-Smale system.

1. Introduction:

Collective coordinated motion of autonomous self-propelled agents with self-organization into robust patterns appears in many applications ranging from animal herding to the emergence of common languages in primitive societies [31]. Apart from their biological and evolutionary relevance, collective phenomena play a prominent role in many other scientific disciplines, such as robotics, control theory, economics, and the social sciences [4, 10, 35, 26]. In this paper we study the interplay of noise and delay on collective behavior. We investigate a modification of the well-known Cucker–Smale model [5, 6] with multiplicative noise and reaction delays. We consider N □ N autonomous agents located in a one-dimensional physical space. The agents are described by their phase-space coordinates (xi(t), vi(t)) □ R2, i = 1, 2,...,N, where xi ≡ xi(t) □ R and vi ≡ vi(t) □ R are the time-dependent position and velocity, respectively, of the ith agent. The (fixed) reaction delay will be denoted by $\tau \geq 0$, and we adopt the following notational convention. Convention 1. Throughout the paper, we denote by xi the position xi evaluated at time t, i.e., xi = xi(t), and by xi the same quantity evaluated at time $t - \tau$, i.e.,

xi = xi(t − τ). The same holds for the velocities vi = vi(t) and vi = vi(t − τ). We will also write x = (x1, x2,...,xN) □ RN (resp., v = (v1, v2,...,vN) □ RN) for the vectors of locations (resp., velocities) of the agents.

The system of equations that we will study is the following system of delayed Itˆo stochastic differential equations:

$$(1.1)\qquad \mathrm{d}x_i = v_i\,\mathrm{d}t,$$

$$(1.2)\qquad \mathrm{d}v_i = \frac{\lambda}{N}\sum_{j=1}^{N}\psi(|\widetilde{x}_i-\widetilde{x}_j|)\,(\widetilde{v}_j-\widetilde{v}_i)\,\mathrm{d}t + \frac{\sigma_i}{N}\sum_{j=1}^{N}\psi(|\widetilde{x}_i-\widetilde{x}_j|)\,(\widetilde{v}_j-\widetilde{v}_i)\,\mathrm{d}B_i^t$$

for i = 1, 2,...,N. The parameters λ > 0 and σi □ R, i = 1, 2,...,N, measure the coupling and noise strength, respectively, and dBt i , i = 1, 2,...,N, are independent white noise scalars. The function ψ : [0, ∞) → [0, ∞) models the communication rate between agents and is assumed to depend on their mutual distance. We note that the scaling by N −1 in (1.2) is significant for obtaining a Vlasov-type kinetic equation in the mean-field limit N → ∞; see, for example, [14]. Our aim is to investigate (1.1)–(1.2) for general values of reaction delay τ and noise strength parameters σi, i = 1, 2,...,N.

The standard Cucker–Smale model [5, 6] is a special case of (1.1)–(1.2) with σi = 0 and τ = 0. It was introduced and studied in the seminal papers [5, 6], originally as a model for language evolution. Later the interpretation as a model for flocking in animals (birds) prevailed. In general, the term flocking refers to the phenomena where autonomous agents reach a consensus based on limited environmental information and simple rules. The communication rate ψ introduced in [5, 6] and most of the subsequent papers is of the form

$$(1.3)\qquad \psi(s) = \frac{1}{(1+s^2)^{\beta}}, \quad \text{where } \beta \geq 0.$$

The Cucker–Smale model is a simple relaxation-type model that reveals a phase transition depending on the intensity of communication between agents. If β < 1/2, then the model exhibits so-called unconditional flocking, where for every initial configuration the velocities vi(t) converge to a common consensus value. On the other hand, with β ≥ 1/2 the flocking is conditional; i.e., the asymptotic behavior of the system depends on the value of λ and on the initial configuration. This result was first proved in [5, 6] using tools from graph theory (spectral properties of graph Laplacian), and slightly later reproved in [14] by means of elementary calculus. Another proof was provided in [13], based on a bound by a system of dissipative differential inequalities, and, finally, the proof in [3] is based on bounding the maximal velocity.

Various modifications of the classical Cucker–Smale model have been considered. For instance, the case of singular communication rates ψ(s)=1/sβ was studied in [13, 27]. Motsch and Tadmor [24] scaled the communication rate between the agents in terms of their relative distance, so that their model does not involve any explicit dependence on the number of agents. The dependence of the communication rate on the topological rather than metric distance between agents was introduced in [15]. The influence of additive noise in individual velocity measurements was studied in [12] and [34]. More complicated noise terms can be derived by considering details of interactions of agents with their environment [8, 9]. Stochastic flocking dynamics with multiplicative white noises was considered in [1]. Delays in information processing were considered in [21]; however, their analysis applies only to the Motsch–Tadmor variant of the model. Synchronization and coordination systems with noise and delays were studied also in [16, 17, 18, 28, 29].

In this paper, we are interested in studying the combined influence of multiplicative noise and reaction delays on the asymptotic behavior of the generalized Cucker– Smale system (1.1)–

(1.2). In particular, we derive a sufficient condition in terms of noise intensities σi and delay length τ that guarantees flocking. Our analysis is based on the construction of a Lyapunov functional and an estimate of its decay rate. To prove our main results, we make an additional structural assumption about the matrix of communication rates which, loosely speaking, means that the communication between agents is strong enough.

The paper is organized as follows: In section 2 we adopt certain simplifying assumptions for the model (1.1)–(1.2) that will facilitate its analysis, and define what is meant by flocking in the context of this model. Moreover, we point out that the model includes delayed geometric Brownian motion as a special case, which provides an insight into which qualitative properties may be expected from its solutions. In section 3 we derive a sufficient condition for flocking in terms of the parameters λ, σi, and τ, based on a micro-macro decomposition and construction of a Lyapunov functional. Moreover, as a by-product of our analysis, we provide a new result about the asymptotic behavior of delayed geometric Brownian motion. Section 4 is devoted to a systematic numerical study of the model. First, we focus on simulation of delayed geometric Brownian motion; in particular, we study the dependence of its asymptotic behavior on the delay and noise levels. Then, we perform the same study for system (1.1)–(1.2). This leads to the interesting observation that, for weak coupling and small noise levels, the introduction of intermediate delays may facilitate flocking. A systematic study of this effect concludes the paper.

2. Model simplifications. In the generic setting, the communication rates ψ(|xi − xj |) in (1.2) are functions of the mutual distances between the agents. However, the analysis in section 3 is based on a certain structural assumption about the communication matrix ψij = ψ(|xi − xj |), and the particular form of the dependence on the mutual distances is irrelevant. This structural assumption is not needed in section 4, where we present a systematic numerical study of the general model (1.1)– (1.2).

We consider the rates ψij = ψij (t) as given adapted stochastic processes, so that (1.2) decouples from (1.1). Moreover, we assume that ψij are uniformly bounded,

$$0 < \psi_{ij}(t) = \psi_{ji}(t) \le 1 \qquad \text{for } t \ge -\tau,\ i,j = 1,2,\dots,N, \quad \text{almost surely.} \tag{2.1}$$

Thus, we finally arrive at the stochastic system of delayed differential equations that we will study analytically in section 3,

$$\mathrm{d}v_i = \frac{\lambda}{N}\sum_{j=1}^{N}\widetilde{\psi}_{ij}\,\left(\widetilde{v}_j - \widetilde{v}_i\right)\mathrm{d}t + \frac{\sigma_i}{N}\sum_{j=1}^{N}\widetilde{\psi}_{ij}\,\left(\widetilde{v}_j - \widetilde{v}_i\right)\mathrm{d}B_i^t \tag{2.2}$$

for i = 1, 2,...,N, with the agreed notation ψij = ψij (t − τ). The system is supplemented with the deterministic constant initial datum v0 □ RN ,

$$v_i(t) \equiv v_i^0 \qquad \text{for } t \in (-\tau, 0],\ i = 1,2,\dots,N. \tag{2.3}$$

Let us note that we interpret the noise term in (2.2) in terms of the Itˆo calculus [25, 22].

Theorem 2.1. The stochastic delay differential system (2.2) with initial condition (2.3) admits a unique global solution v = v(t) on [−τ, ∞), which is an adapted process with E T −τ |v(t)| 2 dt < ∞ for all T < ∞, i.e., a martingale.

Proof. The proof follows directly from Theorem 3.1 of [22] and the subsequent remark on p. 157 there. Indeed, (2.2) is of the form

$$\mathrm{d}\mathbf{v}(t) = F(t, \mathbf{v}(t-\tau))\,\mathrm{d}t + G(t, \mathbf{v}(t-\tau))\,\mathrm{d}B^t$$

for suitable functions F and G. In particular, the right-hand side is independent of the present state v(t), so that the solution can be constructed by the method of steps. The second order moment is bounded on (−τ,T) because of the linear growth of the right-hand side of (2.2) in v.

We now define the property of asymptotic flocking for the solutions of (2.2)–(2.3).

Definition 2.2. We say that system (2.2) exhibits asymptotic flocking if the solution (v(t))t≥0 for any initial condition (2.3) satisfies

$$\lim_{t\to\infty} \mathbb{E}[v_i(t) - v_j(t)] = 0 \qquad \textit{for all } i, j = 1, 2, \ldots, N,$$

where E[·] denotes the expected value of a stochastic process.

2.1. Simplified case with ψ ≡ 1. To get an intuition of what qualitative properties we may expect from the solutions of (2.2), we consider the case when the communication rate is constant, i.e., ψij ≡ 1. We also assume that σi is equal to the same constant σ □ R for all i = 1, 2,...,N, i.e., σi ≡ σ, and, moreover, that v0 i = v0 for some v0 □ R and all i = 1, 2,...,N. Then, defining Vc(t) := 1 N N i=1 vi(t), we obtain

$$\mathrm{d}V_c = \frac{\sigma}{N}\sum_{i=1}^{N}\left(\widetilde{V}_c - \widetilde{v}_i\right)\mathrm{d}B_i^t.$$

Since, by assumption, Vc(t)−vi(t) ≡ 0 for t □ (−τ, 0], we have Vc(t) ≡ v0 for all t ≥ 0. Consequently, (2.2) decouples into N copies of the delayed SDE

$$\mathrm{d}w = -\lambda\,\widetilde{w}\,\mathrm{d}t - \sigma\,\widetilde{w}\,\mathrm{d}B^t, \tag{2.4}$$

where we denote w := vi − v0 for any i = 1, 2,...,N. We are not aware of any results concerning the asymptotic behavior of (2.4). The method developed in [2] suggests that

$$\lim_{t\to\infty} \mathbb{E}\left[|w(t)|^2\right] = 0 \qquad \text{if and only if} \qquad \int_0^\infty r_\lambda(t)^2\,\mathrm{d}t < \frac{1}{\sigma^2},$$

i.e., formally, rλ solves (2.5) subject to the initial condition w(t) = χ{0}(t) for t □ (−τ, 0]. The fundamental solution rλ can be constructed by the method of steps [30]; however, evaluation of its L2(0, ∞)-norm is an open problem. From this point of view, the analysis carried out in section 3 provides new and valuable information about the asymptotics of (2.4); see section 3.4. Let us note that setting τ = 0 in the above criterion recovers the well-known result about

geometric Brownian motion [25]: the mean-squared fluctuation E[|w(t)| 2] tends to zero if and only if σ2 < 2λ.

Finally, for the convenience of the reader, we give an overview of the qualitative behavior of solutions to (2.5) with λ > 0, subject to a constant nonzero initial datum (see, e.g., Chapter 2 of [30]), as follows: • If λτ ≤ 1/e, the solution monotonically converges to zero as t → ∞; hence no oscillations occur.

• If 1/e < λτ < π/2, oscillations appear, however, with asymptotically vanishing amplitude. • If λτ = π/2, periodic solutions exist.

• If λτ > π/2, the amplitude of the oscillations diverges as t → ∞.

Hence, we conclude that the (over)simplified model (2.5), corresponding to the delayed Cucker–Smale system with ψ ≡ 1 and no noise, exhibits flocking if and only if λτ < π/2. In the next section we derive a sufficient condition for flocking for the model (2.2) with given communication rates ψij satisfying (2.1). **3. Sufficient condition for flocking.** In this section we derive a sufficient condition for flocking in (2.2) according to Definition 2.2. Our analysis will be based on a construction of a Lyapunov functional that will imply decay of velocity fluctuations for suitable parameter values. However, we will have to adopt an additional structural assumption on the matrix of communication rates (ψij)N i,j=1.

Before we proceed, let us briefly point out the mathematical difficulties that arise due to the introduction of delay and noise into the Cucker–Smale system. The "traditional" proofs of flocking, for instance [5, 6, 14, 13], rely on the monotone decay of the kinetic energy (velocity fluctuations) of the form

$$\frac{\mathrm{d}}{\mathrm{d}t}\sum_{i=1}^{N}|v_i|^2 = -\frac{\lambda}{N}\sum_{i=1}^{N}\sum_{j=1}^{N}\psi_{ij}|v_i - v_j|^2 \le 0.$$

However, this approach fails if processing delays are introduced, since for (1.2) without noise (i.e., all σi = 0) we have

$$\frac{\mathrm{d}}{\mathrm{d}t}\sum_{i=1}^{N}|v_i|^2 = -\frac{\lambda}{N}\sum_{i=1}^{N}\sum_{j=1}^{N}\widetilde{\psi}_{ij}(v_i - v_j)\cdot(\widetilde{v}_i - \widetilde{v}_j).$$

One then expects the product (vi − vj) · (vi − vj) to be nonnegative for τ > 0 small enough; however, it is not clear how to prove this hypothesis. The introduction of noise leads to additional difficulties—in particular, the classical bootstrapping argument [5, 6, 13] for fluctuations in velocity fails in this case. Much as in [12], we circumvent this problem by adopting, in addition to the boundedness (2.1), a structural assumption about the matrix of communication rates. We define the Laplacian matrix A(t) □ RN×N by

$$\mathbb{A}_{ij} := -\psi_{ij} \quad \text{for } i \neq j, \qquad \mathbb{A}_{ii} := \sum_{j\neq i}\psi_{ij}, \tag{3.1}$$

and note that A is symmetric, diagonally dominant with nonnegative diagonal entries; thus it is positive semidefinite and has real nonnegative eigenvalues. Due to its Laplacian structure,

its smallest eigenvalue is zero [5]. Let us denote its second smallest eigenvalue (the Fiedler number) by μ2(t). Our structural assumption is that there exists an > 0 such that

$$\mu_2(t) \geq \ell > 0 \quad \text{for } t > 0, \quad \text{almost surely.} \tag{3.2}$$

This can be guaranteed, for instance, by assuming that the communication rates are uniformly bounded away from zero, ψij (t) ≥ ¯ ψ > 0, since there exists a constant c > 0 such that μ2(t) ≥ c ¯ ψ; see Proposition 2 in [5]. Moreover, we assume that the matrix of communication rates is uniformly Lipschitz continuous in the Frobenius norm; in particular, there exists a constant L > 0 such that

$$\left\| \mathbb{A} - \widetilde{\mathbb{A}} \right\|_F \leq L\tau \quad \text{for } t \geq 0, \tag{3.3}$$

with the notation A := A(t), A := A(t − τ) and where · F denotes the Frobenius matrix norm. Then, with the definition (3.1), we put (2.2) into the form

$$\mathrm{d}v_i = -\frac{\lambda}{N}(\widetilde{\mathbb{A}}\widetilde{\mathbf{v}})_i \,\mathrm{d}t + \frac{\sigma_i}{N}(\widetilde{\mathbb{A}}\widetilde{\mathbf{v}})_i \,\mathrm{d}B_i^t, \qquad i = 1, 2, \ldots, N. \tag{3.4}$$

Our main result is the following.

Theorem 3.1. Let A be given by (3.1) satisfying (2.1), (3.2), and (3.3). Let the parameters λ > 0 and σ2 max := max{σ2 1, σ2 2,...,σ2 N } satisfy

$$\sigma_{\max}^2 < \lambda. \tag{3.5}$$

Then there exists a critical delay τc = τc(λ, σmax, L,) > 0, independent of N, such that for every 0 ≤ τ<τc the system (3.4) exhibits flocking in the sense of Definition 2.2.

Moreover, if the matrix of communication rates A is constant, i.e., (3.3) holds with L = 0, then τc is of the form

$$\tau_c = \frac{1}{\lambda^2}\left(-\sigma_{\max}^2 + \sqrt{\sigma_{\max}^4 + \frac{1}{12}(\lambda - \sigma_{\max}^2)^2} \right). \tag{3.6}$$

Remark 1. The system (3.4) with constant communication matrix A can be seen as a linearization of the system (1.1)–(1.2) about the equilibrium vi ≡ v0 for i = 1, 2,...,N with some v0 □ R. Note that in this case the formula (3.6) for the critical delay τc does not depend on the particular value of in (3.2).

3.1. Micro-macro decomposition. We introduce a micro-macro decomposition [14, 12] which splits (3.4) into two parts: macroscopic, which describes the coarse-scale dynamics, and microscopic, which describes the fine-scale dynamics. The macroscopic part for the solution is set to be the mean velocity Vc(t),

$$V_c(t) := \frac{1}{N}\sum_{i=1}^{N} v_i(t). \tag{3.7}$$

The microscopic variables are then taken as the fluctuations around their mean values,

$$w_i(t) := v_i(t) - V_c(t) \quad \text{for } i = 1, 2, \dots, N. \tag{3.8}$$

We denote w(t)=(w1, w2,...,wN) □ RN . Then we have

$$\mathbf{w}(t) = \mathbf{v}(t) - V_c(t)\,\mathbf{e}, \qquad \text{where } \mathbf{e} := (1, 1, \dots, 1)^T \in \mathbb{R}^N. \tag{3.9}$$

Since e is the eigenvector of A corresponding to the zero eigenvalue, we have Aw = Av.

Then (3.4) can be rewritten as follows:

$$dw_i = -\frac{\lambda}{N}(\widetilde{\mathbb{A}}\widetilde{\mathbf{w}})_i\,dt + \frac{\sigma_i}{N}(\widetilde{\mathbb{A}}\widetilde{\mathbf{w}})_i\,dB_i^t - dV_c. \tag{3.10}$$

The macroscopic variable Vc satisfies the following lemma.

Lemma 3.2. Let (v(t))t≥0 be a solution of (2.2) subject to the deterministic constant initial datum (2.3). Then E[Vc(t)] ≡ Vc(0) for t ≥ 0 and E _x0007_ T −τ |Vc(t)| 2 dt < ∞ for all T < ∞.

Proof. The boundedness of E _x0007_ T −τ |Vc(t)| 2 dt follows directly from the definition (3.7) and the martingale property of v(t) provided by Theorem 2.1. Using (3.1), we have

$$\sum_{i=1}^{N}(\widetilde{\mathbb{A}}\widetilde{\mathbf{v}})_i = \mathbf{e}^T\widetilde{\mathbb{A}}\widetilde{\mathbf{v}} = 0.$$

Summing equations (3.4), i = 1, 2,...,N, using (3.7) and Aw = Av, we obtain that

the macroscopic dynamics is governed by the system

$$dV_c = \frac{1}{N^2}\sum_{i=1}^{N}\sigma_i(\widetilde{\mathbb{A}}\widetilde{\mathbf{w}})_i\,dB_i^t. \tag{3.11}$$

After integration in time this implies

$$\mathbb{E}[V_c(t)] = V_c(0) + \frac{1}{N^2}\sum_{i=1}^{N}\sigma_i\,\mathbb{E}\left[\int_0^t(\mathbb{A}(s-\tau)\mathbf{w}(s-\tau))_i\,dB_i^s\right] \qquad \text{for } t \geq 0.$$

Since f(s) := (A(s − τ)w(s − τ))i is a martingale, we have E _x0007_ t 0 f(s) dBs i = 0 (see [22, Theorem 5.8, p. 22]). Thus we obtain E[Vc(t)] ≡ Vc(0).

Remark 2. Note that (3.10) and (3.11) are expressed in terms of the w-variables only, and so they form a closed system, which is equivalent to (3.4). Clearly, due to (3.8), we have w · e = N i=1 wi ≡ 0. Consequently, it is natural to introduce the decomposition RN = e□ e□, where e is given by (3.9). We then have w(t) □ e□ for all t ≥ 0.

Lemma 3.3. Let A □ RN×N , N ≥ 2, be the matrix defined in (3.1), and assume that (2.1) and (3.2) hold. Then we have the following:

(a) The maximal eigenvalue of A is bounded by 2 (N − 1).

(b) We have |Au| 2 ≤ 2 (N − 1) uT Au for any vector u □ RN .

(c) We have |w| 2 ≤ wT Aw ≤ 2 (N − 1)|w| 2 for any vector w □ e□.

(d) For any vectors u, w □ e□ and δ > 0 we have

$$\mathbf{u}^T\mathbb{A}\mathbf{w} \le \frac{1}{2\delta}\,\mathbf{u}^T\mathbb{A}\mathbf{u} + \frac{\delta}{2}\,\mathbf{w}^T\mathbb{A}\mathbf{w}.$$

Proof. (a) The claim follows from the Gershgorin circle theorem. Indeed, since 0 < ψij ≤ 1, the diagonal entries satisfy 0 ≤ Aii ≤ N − 1, and j_x0007_=i |Aij | = Aii for all i = 1, 2,...,N.

(b) The smallest eigenvalue of A is zero with the corresponding eigenvector e. The second smallest eigenvalue μ2 (the Fiedler number) is assumed to be positive

by (3.2). Thus, A is a symmetric positive operator on the space e □, and there exists an orthonormal basis of e □ composed of eigenvectors ξ2, ξ3,..., ξN of A corresponding to the positive eigenvalues μ2, μ3,...,μN . Then, every vector u □ RN can be decomposed as

$$\mathbf{u} = \frac{(\mathbf{u}\cdot\mathbf{e})\,\mathbf{e}}{|\mathbf{e}|^2} + \sum_{i=2}^{N}(\mathbf{u}\cdot\boldsymbol{\xi}_i)\,\boldsymbol{\xi}_i. \tag{3.12}$$

Thus, due to the above bound on the eigenvalues 0 ≤ μi ≤ 2(N − 1), we have

$$|\mathbb{A}\mathbf{u}|^2 = \sum_{i=2}^{N}(\mathbf{u}\cdot\boldsymbol{\xi}_i)^2\mu_i^2 \le 2\,(N-1)\sum_{i=2}^{N}(\mathbf{u}\cdot\boldsymbol{\xi}_i)^2\mu_i = 2\,(N-1)\,\mathbf{u}^T\mathbb{A}\mathbf{u}.$$

(c) If $\mathbf{w} \in \langle\mathbf{e}\rangle^{\perp}$, then (3.12) implies

$$\mathbf{w} = \sum_{i=2}^{N}(\mathbf{w}\cdot\boldsymbol{\xi}_i)\,\boldsymbol{\xi}_i \qquad \text{and} \qquad \mathbf{w}^T\mathbb{A}\mathbf{w} = \sum_{i=2}^{N}(\mathbf{w}\cdot\boldsymbol{\xi}_i)^2\mu_i.$$

Since nonzero eigenvalues are bounded from below by (using (3.2)) and from above by part (a) of this lemma, we obtain

$$(\mathbf{u}^T\mathbb{A}\mathbf{u})^{\frac{1}{2}}(\mathbf{w}^T\mathbb{A}\mathbf{w})^{\frac{1}{2}} \le \frac{1}{2\delta}\,\mathbf{u}^T\mathbb{A}\mathbf{u} + \frac{\delta}{2}\,\mathbf{w}^T\mathbb{A}\mathbf{w}. \qquad \square$$

3.2. Lyapunov functional. The proof of Theorem 3.1 relies on estimating the decay rate of the following Lyapunov functional for (3.10)–(3.11):

$$\mathscr{L}(t) := |\mathbf{w}(t)|^2 + \frac{q}{N^2}\int_{t-\tau}^{t}|\mathbb{A}(s)\,\mathbf{w}(s)|^2\,\mathrm{d}s + \frac{p}{N^2}\int_{t-\tau}^{t}\int_{\theta}^{t}|\mathbb{A}(s-\tau)\,\mathbf{w}(s-\tau)|^2\,\mathrm{d}s\,\mathrm{d}\theta, \tag{3.13}$$

where p, q are positive constants depending on λ, τ, and σi.

Lemma 3.4. Let the assumptions of Theorem 3.1 be satisfied. Then there exist positive constants p, q, and ε such that for every solution (w(t))t≥0 of (3.10)–(3.11) the Lyapunov functional (3.13) satisfies

ISSN PRINT 2319 1775 Online 2320 7876
 UGC CARE Listed (Group -I) Journal Volume 11, Iss 01, 2022

$$\frac{\mathrm{d}}{\mathrm{d}t}\,\mathbb{E}[\mathscr{L}(t)] \le -\frac{\varepsilon}{N}\,\mathbb{E}\left[\mathbf{w}^T\widetilde{\mathbb{A}}\mathbf{w}\right]. \tag{3.14}$$

Proof. We apply the Itˆo formula to calculate dwi(t)2. Note that the Itˆo formula holds in its usual form also for systems of delayed SDE; see [11, p. 32] and [20, 7, 23]. Therefore, we obtain

$$\begin{aligned}\mathrm{d}w_i(t)^2 = &-\frac{2\lambda}{N}w_i(\widetilde{\mathbb{A}}\widetilde{\mathbf{w}})_i\,\mathrm{d}t + \frac{2\sigma_i}{N}w_i(\widetilde{\mathbb{A}}\widetilde{\mathbf{w}})_i\,\mathrm{d}B_i^t - 2w_i\,\mathrm{d}V_c\\ &+\frac{\sigma_i^2}{N^2}(\widetilde{\mathbb{A}}\widetilde{w})_i^2\,\mathrm{d}t + \frac{1}{N^4}\sum_{j=1}^N\sum_{k=1}^N\sigma_j\sigma_k(\widetilde{\mathbb{A}}\widetilde{w})_j(\widetilde{\mathbb{A}}\widetilde{w})_k\,\mathrm{d}B_j^t\,\mathrm{d}B_k^t\\ &-2\left(\frac{\sigma_i}{N}(\widetilde{\mathbb{A}}\widetilde{w})_i\,\mathrm{d}B_i^t\right)\mathrm{d}V_c.\end{aligned}$$

With the identity dBt j dBt k = δjk dt (formula (6.11) on p. 36 of [22]), we have

$$\frac{1}{N^4}\sum_{j=1}^N\sum_{k=1}^N\sigma_j\sigma_k(\widetilde{\mathbb{A}}\widetilde{w})_j(\widetilde{\mathbb{A}}\widetilde{w})_k\,\mathrm{d}B_j^t\,\mathrm{d}B_k^t = \frac{1}{N^4}\sum_{j=1}^N\sigma_j^2(\widetilde{\mathbb{A}}\widetilde{w})_j^2\,\mathrm{d}t.$$

Consequently, summing over i, using w · e and the identity

$$\sum_{i=1}^N\left(\frac{\sigma_i}{N}(\widetilde{\mathbb{A}}\widetilde{w})_i\,\mathrm{d}B_i^t\right)\mathrm{d}V_c = \frac{1}{N^3}\sum_{i=1}^N\sigma_i^2(\widetilde{\mathbb{A}}\widetilde{w})_i^2\,\mathrm{d}t,$$

we obtain

$$\mathrm{d}|\mathbf{w}(t)|^2 = \left(-\frac{2\lambda}{N}\mathbf{w}^T\widetilde{\mathbb{A}}\widetilde{\mathbf{w}} + \frac{N-1}{N^3}\sum_{i=1}^N\sigma_i^2(\widetilde{\mathbb{A}}\widetilde{\mathbf{w}})_i^2\right)\mathrm{d}t + \frac{2}{N}\sum_{i=1}^N\sigma_i w_i(\widetilde{\mathbb{A}}\widetilde{\mathbf{w}})_i\,\mathrm{d}B_i^t.$$

Consequently, we have

$$\begin{aligned}\mathrm{d}\mathscr{L}(t) = &\left(-\frac{2\lambda}{N}\mathbf{w}^T\widetilde{\mathbb{A}}\widetilde{\mathbf{w}} + \frac{N-1}{N^3}\sum_{i=1}^N\sigma_i^2(\widetilde{\mathbb{A}}\widetilde{\mathbf{w}})_i^2\right)\mathrm{d}t + \frac{2}{N}\sum_{i=1}^N\sigma_i w_i(\widetilde{\mathbb{A}}\widetilde{\mathbf{w}})_i\,\mathrm{d}B_i^t\\ &+\frac{q}{N^2}\left(|\mathbb{A}\mathbf{w}|^2 - |\widetilde{\mathbb{A}}\widetilde{\mathbf{w}}|^2\right)\mathrm{d}t + \frac{p}{N^2}\left(\tau|\widetilde{\mathbb{A}}\widetilde{\mathbf{w}}|^2 - \int^t|\mathbb{A}\mathbf{w}(s-\tau)|^2\,\mathrm{d}s\right)\mathrm{d}t.\end{aligned} \tag{3.15}$$

Our goal is to estimate d dtE[L (t)] from above. First, we note that by the elementary property of the Itˆo integral [22, Theorem 5.8, p. 22],

$$\mathbb{E}\left[\frac{1}{N}\sum_{i=1}^N\sigma_i w_i(\widetilde{\mathbb{A}}\widetilde{\mathbf{w}})_i\,\mathrm{d}B_i^t\right] = 0.$$

For the first term of the right-hand side in (3.15), we write

$$-\frac{2\lambda}{N}\mathbf{w}^T\widetilde{\mathbb{A}}\widetilde{\mathbf{w}} = -\frac{2\lambda}{N}\mathbf{w}^T\widetilde{\mathbb{A}}\mathbf{w} + \frac{2\lambda}{N}\mathbf{w}^T\widetilde{\mathbb{A}}(\mathbf{w}-\widetilde{\mathbf{w}})$$

and apply Lemma 3.3(d) with δ > 0

$$\frac{2\lambda}{N}\mathbf{w}^T\widetilde{\mathbb{A}}(\mathbf{w}-\widetilde{\mathbf{w}}) \le \frac{\lambda\delta^{-1}}{N}\mathbf{w}^T\widetilde{\mathbb{A}}\mathbf{w} + \frac{\lambda\delta}{N}(\mathbf{w}-\widetilde{\mathbf{w}})^T\widetilde{\mathbb{A}}(\mathbf{w}-\widetilde{\mathbf{w}}).$$

Using Lemma 3.3(c), we have

$$\frac{\lambda\delta}{N}(\mathbf{w}-\widetilde{\mathbf{w}})^T\widetilde{\mathbb{A}}(\mathbf{w}-\widetilde{\mathbf{w}}) \le 2\lambda\delta\frac{N-1}{N}|\mathbf{w}-\widetilde{\mathbf{w}}|^2. \tag{3.16}$$

Now we write for w − w , componentwise, using (3.10),

$$\begin{aligned} w_i - \widetilde{w}_i &= \int_{t-\tau}^{t} \mathrm{d}w_i(s) \\ &= -\frac{\lambda}{N}\int_{t-\tau}^{t}(\mathbb{A}(s-\tau)w(s-\tau))_i\,\mathrm{d}s + \frac{\sigma_i}{N}\int_{t-\tau}^{t}(\mathbb{A}(s-\tau)w(s-\tau))_i\,\mathrm{d}B_i^s \\ &\quad -\int_{t-\tau}^{t}\mathrm{d}V_c(s). \end{aligned}$$

Thus, we have for the expectation of the square

$$\begin{aligned} \mathbb{E}|w_i-\widetilde{w}_i|^2 \le\ & 3\,\mathbb{E}\left[\frac{\lambda}{N}\int_{t-\tau}^{t}(\mathbb{A}(s-\tau)\mathbf{w}(s-\tau))_i\,\mathrm{d}s\right]^2 \\ & +3\,\mathbb{E}\left[\frac{\sigma_i}{N}\int_{t-\tau}^{t}(\mathbb{A}(s-\tau)\mathbf{w}(s-\tau))_i\,\mathrm{d}B_i^s\right]^2 \\ & +3\,\mathbb{E}\left[\int_{t-\tau}^{t}\mathrm{d}V_c(s)\right]^2. \end{aligned}$$

An application of the Cauchy–Schwarz inequality and Fubini's theorem for the first term of the right-hand side yields

$$3\,\mathbb{E}\left[\frac{\lambda}{N}\int_{t-\tau}^{t}(\mathbb{A}(s-\tau)\mathbf{w}(s-\tau))_i\,\mathrm{d}s\right]^2 \le \frac{3\lambda^2}{N^2}\tau\int_{t-\tau}^{t}\mathbb{E}\left[|(\mathbb{A}(s-\tau)\mathbf{w}(s-\tau))_i|^2\right]\mathrm{d}s.$$

For the second term we use the fundamental property of the Itˆo integral [22, Theorem 5.8, p. 22],

$$3\,\mathbb{E}\left[\frac{\sigma_i}{N}\int_{t-\tau}^{t}(\mathbb{A}(s-\tau)\mathbf{w}(s-\tau))_i\,\mathrm{d}B_i^s\right]^2 = \frac{3\sigma_i^2}{N^2}\int_{t-\tau}^{t}\mathbb{E}\left[|(\mathbb{A}(s-\tau)\mathbf{w}(s-\tau))_i|^2\right]\mathrm{d}s.$$

Similarly, the third term is estimated as

ISSN PRINT 2319 1775 Online 2320 7876
 UGC CARE Listed (Group -I) Journal Volume 11, Iss 01, 2022

$$3\,\mathbb{E}\left[\int_{t-\tau}^{t} \mathrm{d}V_c(s)\right]^2 = \frac{3}{N^4}\,\mathbb{E}\left[\sum_{j=1}^{N}\int_{t-\tau}^{t} \sigma_j(\mathbb{A}(s-\tau)\mathbf{w}(s-\tau))_j\,\mathrm{d}B_j^s\right]^2$$
$$\leq \frac{3}{N^3}\sum_{j=1}^{N}\mathbb{E}\left[\int_{t-\tau}^{t} \sigma_j(\mathbb{A}(s-\tau)\mathbf{w}(s-\tau))_j\,\mathrm{d}B_j^s\right]^2$$
$$\leq \frac{3\sigma_{\max}^2}{N^3}\sum_{j=1}^{N}\int_{t-\tau}^{t}\mathbb{E}\left[|(\mathbb{A}(s-\tau)\mathbf{w}(s-\tau))_j|^2\right]\,\mathrm{d}s.$$

Thus, we get from (3.16), estimating N−1 N ≤ 1,

$$\frac{\lambda\,\delta}{N}\mathbb{E}\left[(\mathbf{w}-\widetilde{\mathbf{w}})^T\widetilde{\mathbb{A}}(\mathbf{w}-\widetilde{\mathbf{w}})\right] \leq \frac{6\,\lambda\,\delta}{N^2}\,(\lambda^2\tau+2\sigma_{\max}^2)\sum_{i=1}^{N}\int_{t-\tau}^{t}\mathbb{E}\left[|(\mathbb{A}(s-\tau)\mathbf{w}(s-\tau))_i|^2\right]\mathrm{d}s.$$

An application of Lemma 3.3(b) gives

$$\frac{q}{N^2}\,\mathbb{E}[|\mathbb{A}\mathbf{w}|^2] \leq \frac{2\,q\,(N-1)}{N^2}\,\mathbb{E}[\mathbf{w}^T\mathbb{A}\mathbf{w}] \leq \frac{2\,q}{N}\,\mathbb{E}[\mathbf{w}^T\mathbb{A}\mathbf{w}].$$

To balance this term with −2λ N wT Aw, we use assumption (3.3) and Lemma 3.3(c) in

$$\mathbf{w}^T\mathbb{A}\mathbf{w} = \mathbf{w}^T(\mathbb{A}-\widetilde{\mathbb{A}})\mathbf{w} + \mathbf{w}^T\widetilde{\mathbb{A}}\mathbf{w}$$
$$\leq L\tau\mathbf{w}^T\mathbf{w} + \mathbf{w}^T\widetilde{\mathbb{A}}\mathbf{w} \leq \left(L\ell^{-1}\tau+1\right)\mathbf{w}^T\widetilde{\mathbb{A}}\mathbf{w}.$$

Collecting all the terms in (3.15) finally leads to

$$\frac{\mathrm{d}}{\mathrm{d}t}\,\mathbb{E}[\mathscr{L}(t)] \leq \frac{1}{N}\left[-2\,\lambda+\lambda\,\delta^{-1}+2\,q\left(L\ell^{-1}\tau+1\right)\right]\mathbb{E}[\mathbf{w}^T\widetilde{\mathbb{A}}\mathbf{w}]$$
$$+\frac{1}{N^2}\left(\sigma_{\max}^2+p\,\tau-q\right)\mathbb{E}|\widetilde{\mathbb{A}}\widetilde{\mathbf{w}}|^2$$
$$+\frac{1}{N^2}\left(6\,\lambda\,\delta\,(\lambda^2\tau+2\sigma_{\max}^2)-p\right)\int_{t-\tau}^{t}\mathbb{E}|\mathbb{A}(s-\tau)\mathbf{w}(s-\tau)|^2\,\mathrm{d}s.$$

We set

$$p = 6\,\lambda\,\delta\,(\lambda^2\tau+2\sigma_{\max}^2), \qquad q = \sigma_{\max}^2 + p\,\tau; \tag{3.17}$$

then the above expression simplifies to

$$\frac{\mathrm{d}}{\mathrm{d}t}\,\mathbb{E}[\mathscr{L}(t)] \leq \frac{1}{N}\left[-2\,\lambda+\lambda\,\delta^{-1}+2\,q\left(L\ell^{-1}\tau+1\right)\right]\mathbb{E}[\mathbf{w}^T\widetilde{\mathbb{A}}\mathbf{w}]. \tag{3.18}$$

We want −2 λ + λ δ−1 + 2 q L −1τ + 1_x0005_ < 0. Substituting (3.17) into this inequality leads to a third order polynomial inequality in τ. This polynomial has all positive coefficients but the zero order one, which is c0 := 2σ2 max + δ−1λ − 2λ. If (3.5) is satisfied, then choosing δ > 0 such that

$$\delta^{-1} < 2\lambda^{-1}(\lambda-\sigma_{\max}^2)$$

makes c0 negative. Consequently, there exists a τc > 0 such that for any 0 ≤ τ<τc,

$$-2\lambda + \lambda\delta^{-1} + 2q\left(L\ell^{-1}\tau + 1\right) = -\varepsilon < 0.$$

and we have to find τ such that −2 λ + λ δ−1 + 2 q < 0. Again, substituting (3.17) for p and q leads to

$$\tau < \frac{\lambda\,(2-\delta^{-1}) - 2\,\sigma_{\max}^2}{12\,\lambda\,\delta\,(\lambda^2\tau + 2\sigma_{\max}^2)}. \tag{3.19}$$

The maximum value of the right-hand side is obtained for δ = λ(λ − σ2 max)−1, which is positive because of the first inequality in (3.6). Substituting δ = λ(λ − σ2 max)−1 into (3.19), we obtain

$$\tau < \frac{(\lambda - \sigma_{\max}^2)^2}{12\,\lambda^2\,(\lambda^2\tau + \sigma_{\max}^2)}.$$

Finally, resolving in τ leads to

$$\tau < \frac{1}{\lambda^2}\left(-\sigma_{\max}^2 + \sqrt{\sigma_{\max}^4 + \frac{1}{12}(\lambda - \sigma_{\max}^2)^2}\right).$$

If the above sharp inequality is satisfied, there exists an ε > 0 such that −ε = −2 λ + λ δ−1 + 2 q and, consequently, (3.14) holds.

3.3. Proof of Theorem 3.1. An integration of (3.14) in time gives

$$\begin{aligned}\mathbb{E}[|\mathbf{w}|^2(t)] \le \mathbb{E}[\mathscr{L}(t)] &= \mathbb{E}[\mathscr{L}(0)] + \int_0^t \frac{\mathrm{d}}{\mathrm{d}t}\mathbb{E}[\mathscr{L}(s)]\,\mathrm{d}s \\ &\le \mathbb{E}[\mathscr{L}(0)] - \frac{\varepsilon}{N}\int_0^t \mathbb{E}[\mathbf{w}^T(s)\mathbb{A}(s)\mathbf{w}(s)]\,\mathrm{d}s.\end{aligned}$$

An application of Lemma 3.3(c) then gives

$$\mathbb{E}[|\mathbf{w}|^2(t)] \le \mathbb{E}[\mathscr{L}(0)] - \frac{\varepsilon\,\ell}{N}\int_0^t \mathbb{E}[|\mathbf{w}(s)|^2]\,\mathrm{d}s,$$

so that the last integral is convergent as t → ∞, and consequently, limt→∞ E[wi(t)] = 0 for all i = 1, 2,...,N. Using (3.8), we obtain

$$\lim_{t\to\infty} |\mathbb{E}[v_i(t)] - \mathbb{E}[v_j(t)]| = \lim_{t\to\infty} |\mathbb{E}[w_i(t)] - \mathbb{E}[w_j(t)]| = 0,$$

and we conclude that asymptotic flocking in the sense of Definition 2.2 takes place.

Remark 3. The original definition of asymptotic flocking [5, 6] involves, in addition to our Definition 2.2, also the group formation property for (1.1)–(1.2) given by

$$\sup_{t\ge 0} |\mathbb{E}[x_i(t)] - \mathbb{E}[X_c(t)]| < \infty \qquad \text{for all } i = 1, 2, \ldots, N,$$

where Xc(t) := 1 N N i=1 xi(t). The standard way [5, 6, 14, 13] of proving this result would be to estimate

ISSN PRINT 2319 1775 Online 2320 7876
 UGC CARE Listed (Group -I) Journal Volume 11, Iss 01, 2022

$$|\mathbb{E}[x_i(t)] - \mathbb{E}[X_c(t)]| \leq |x_i^0 - X_c(0)| + \int_0^t \mathbb{E}[|w_i(s)|]\,ds$$

and employ a bootstrapping argument to show that _x0007_ ∞ 0 E[|wi(s)|] ds < ∞. However, as noted above, it is not clear how to apply the bootstrapping argument in our setting. Note that we have _x0007_ ∞ 0 E[|wi(s)| 2] ds < ∞, but that does not imply _x0007_ ∞ 0 E[|wi(s)|] ds < ∞.

3.4. Application to asymptotic behavior of delayed geometric Brownian motion. Our analysis provides information about the asymptotic behavior of the delayed geometric Brownian motion (2.4) which is, to the best of our knowledge, new. We just modify the proof of Lemma 3.4 with the obvious simplifications due to the fact that A(t) ≡ 1. This leads to a slight improvement in the flocking condition. Lemma 3.5. Let the parameters λ > 0, σ □ R, and τ ≥ 0 satisfy

$$\sigma^2 < 2\lambda, \qquad \tau < \frac{1}{4\lambda^2}\left(-2\sigma^2 + \sqrt{4\sigma^4 + 2(2\lambda - \sigma^2)^2}\right). \tag{3.20}$$

Then the solutions of the delayed geometric Brownian motion equation (2.4) satisfy

$$\lim_{t\to\infty} \mathbb{E}[|w|^2] = 0.$$

Let us note that the above result is suboptimal for the deterministic case. Indeed, setting σ := 0, equation (3.20) reduces to λτ < √2/2. However, it is known [30] that solutions of the delayed ODE ˙w = −λw asymptotically converge to zero if λτ < π/2. On the other hand, if there is no delay, i.e., τ = 0, the condition (3.20) reduces to σ2 < 2λ, which is the sharp condition for asymptotic vanishing of mean-squared fluctuations of geometric Brownian motion.

4. Numerical experiments. We provide results of numerical experiments for the models considered in this paper with focus on their asymptotic behavior. First, we illustrate that one has to be cautious when interpreting the numerical results as indications about the "true" asymptotic behavior of the solution, because implementations of Monte Carlo algorithms for geometric Brownian motion lead to systematic underestimation of the moments of the true solution; see section 4.1. Keeping this systematic defect in mind, we will resort to weak methods for simulation of our SDEs and study their numerical asymptotic behavior. In section 4.2, we resort to the delayed geometric Brownian motion (2.4), which can be seen as a toy model of (1.1)–(1.2), and find combinations of parameter values that guarantee numerical asymptotic decay of the solution. In section 4.3, we then perform numerical simulations of the velocity alignment system (2.2) with fixed communication rates, and, finally, in section 4.4, we focus on the full system (1.1)–(1.2).

4.1. **Analysis of the Monte Carlo method for geometric Brownian motion.** In this section we estimate the systematic error produced by numerical implementations of the Monte Carlo algorithm for geometric Brownian motion without delay. We show that computer simulations underestimate the mean-squared fluctuations of the process due to the fact that the numerical implementation does not capture large deviations (extreme outliers), and the error grows exponentially in time. Let us consider the one-dimensional Brownian motion with drift,

ISSN PRINT 2319 1775 Online 2320 7876
 UGC CARE Listed (Group -I) Journal Volume 11, Iss 01, 2022

$$(4.1) \qquad dz = (\lambda - \sigma^2/2)\,dt + \sigma\,dB^t, \qquad z(0) = 0.$$

Then, defining $v(t) := \exp[z(t)]$, we have by the Itô formula

$$(4.2) \qquad dv = \lambda v\,dt + \sigma v\,dB^t, \qquad v(0) = 1.$$

For simplicity, we perform a model calculation with $2\lambda = \sigma^2 > 0$, so that

$$(4.3) \qquad dz = \sqrt{2\lambda}\,dB^t, \qquad dv = \lambda v\,dt + \sqrt{2\lambda}\,v\,dB^t.$$

Then, the density $u(t,x)$ of the process z is given by

$$u(t,x) = \frac{1}{\sqrt{4\pi\lambda t}} \exp\left(-\frac{x^2}{4\lambda t}\right).$$

Moreover, we have

$$\mathbb{E}[z(t)] = 0, \qquad \mathbb{E}[z^2(t)] = 2\lambda t, \qquad \mathbb{E}[v(t)] = \exp(\lambda t), \qquad \mathbb{E}[v^2(t)] = \exp(4\lambda t).$$

4.2.

We assume that our numerical scheme produces approximations ¯z of the process z that exclude the extreme outliers; i.e., Prob(|z¯(t)| > α(t)) = 0 for some α = α(t). In particular, we consider a properly scaled cut-off of the density u(t, x) such that the probability of the extreme outliers Prob(|z(t)| > α(t)) remains constant in time. This leads to α(t) = η √ 4 λ t for some η > 0, since

$$\mathrm{Prob}(|z(t)| > \eta\sqrt{4\lambda t}) = 2\int_{\eta\sqrt{4\lambda t}}^{\infty} u(t,x)\,dx = \mathrm{erfc}(\eta),$$

where $\mathrm{erfc}(\eta) = \frac{2}{\sqrt{\pi}}\int_\eta^\infty \exp(-x^2)\,dx$ is the complementary error function. Consequently, we turn $u(t,x)$ into the truncated probability density

$$\bar{u}_\eta(t,x) := \frac{\chi_{[-\alpha(t),\alpha(t)]}(x)}{\mathrm{erf}(\eta)}\,u(t,x),$$

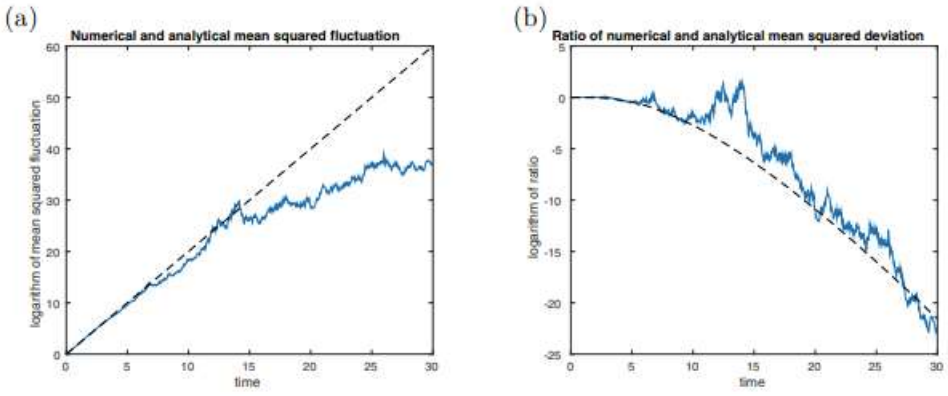

Fig. 1. (a) Logarithm of the simulated mean-squared fluctuations log(E[¯v2(t)]) (solid line) and the analytical result log(E[v2(t)]) = 4 λ t (dashed line). (b) Logarithm of the ratio of simulated and analytically calculated mean-squared fluctuations E[¯v2(t)]/E[v2(t)] (solid line) and the theoretically calculated curve (dashed line) given by the right-hand side of (4.4). The Monte Carlo simulation for z(t) was performed with 106 paths of the process (4.1) with z(0) = 0, λ = 0.5, and σ = 1 on the time interval [0, 30] divided into 103 equidistant sampling points.

where $\chi[-\alpha(t),\alpha(t)]$ is the characteristic function of interval $[-\alpha(t), \alpha(t)]$ and $\mathrm{erf}(\eta) = 1 - \mathrm{erfc}(\eta)$ is the error function. Let us denote by $\bar{z}(t)$ the process with the density $u\bar{}\eta(t, x)$ for a fixed $\eta > 0$, and $\bar{v}(t) := \exp(\bar{z}(t))$. A simple calculation then reveals that

$$\mathbb{E}[\bar{v}^2(t)] = \int_{-\infty}^{\infty} \exp(2x)\, \mathrm{d}\bar{u}_\eta(x) = \frac{\exp(4\,\lambda\, t)}{2\,\mathrm{erf}(\eta)} \left(\mathrm{erfc}\left(-\eta - \sqrt{4\lambda t}\right) - \mathrm{erfc}\left(\eta - \sqrt{4\lambda t}\right)\right).$$

Consequently, since $\mathbb{E}[v^2(t)] = \exp(4\,\lambda\, t)$, the numerical method produces the relative error

$$\frac{\mathbb{E}[\bar{v}^2(t)]}{\mathbb{E}[v^2(t)]} = \frac{\mathrm{erfc}(-\eta - \sqrt{4\lambda t}) - \mathrm{erfc}(\eta - \sqrt{4\lambda t})}{2\,\mathrm{erf}(\eta)}. \tag{4.4}$$

This ratio is equal to one for t = 0. Using the mean value theorem, we obtain the asymptotic behavior of the ratio for large times,

$$\frac{\mathbb{E}[\bar{v}^2(t)]}{\mathbb{E}[v^2(t)]} \approx \frac{2\,\eta}{\sqrt{\pi}\,\mathrm{erf}(\eta)} \exp(-4\lambda t) \qquad \text{as } t \to \infty.$$

Consequently, any implementation of the Monte Carlo method excluding large deviations will underestimate the true value of E[v2(t)] by an exponentially growing factor in time. Let us note that this is also true for any moment of v and with general parameters λ and σ. We illustrate this fact using a numerical simulation. We perform a Monte Carlo simulation in Matlab with 106 paths of the process (4.1) on the time interval [0, T] with T = 30 and 103 equidistant sampling points. We impose the initial condition z(0) = 0 and the parameter values λ = 0.5 and σ = 1. Consequently, z(t) is the Wiener process Bt , and for its numerical approximation $\bar{z}$ we use the built-in Matlab procedure normrnd that generates normally distributed random numbers. We calculate $\bar{v}(t) := \exp(\bar{z}(t))$ and evaluate the mean-squared fluctuations $E[\bar{v}2(t)]$. We plot its logarithm as the solid curve in Figure 1(a), compared to the analytical curve log(E[v2(t)]) = 4 λ t (dashed line). We observe the exponential-in-time divergence of the two curves. This is well described by our formula (4.4), as illustrated

in Figure 1(b). For the calculation of the cut-off parameter η we use the maximal value attained by the actual numerical realization of the stochastic process; i.e., we set $\eta := \max_{t\in(0,T]} |\bar{z}(t)| \sqrt{4\,\lambda\, t}$. We then plot the logarithm of the ratio $E[\bar{v}2(t)]/E[v2(t)]$ and the theoretically calculated curve given by the right-hand side of (4.4). We observe a good match between the two curves.

This systematic discrepancy between the analytical formulas and Monte Carlo simulations originates in the heavy tailed distribution of the geometric Brownian motion and is a well-studied topic; see, e.g., the survey [19]. Importance sampling and rare-event simulation techniques would be the methods of choice to overcome this problem; however, their implementation is beyond the scope of our paper.

4.3. Numerical study of delayed geometric Brownian motion. Using λ = 1, the delayed SDE (2.4) can be equivalently written as

$$\mathrm{d}w = -\tilde{w}\ \mathrm{d}t + \sigma\, \tilde{w}\ \mathrm{d}B^t, \tag{4.5}$$

where $\sigma \geq 0$ and $\tau \geq 0$ are nonnegative parameters. We perform a systematic numerical study of the delayed SDE (4.5) to characterize the asymptotic behavior of its solutions in

dependence on the values of the parameters σ and τ. In particular, we divide the domain [0, 2] × [0, 2] for (σ, τ) into 100 × 100 equidistant (σ, τ)-pairs. For each pair of the parameter values we perform a Monte Carlo simulation for (4.5) with Q = 100 paths over the time interval [0, T] with T = 30 and timestep Δt = 10−3. We impose the constant deterministic initial condition w(t) ≡ 1 for t □ (−τ, 0]. For discretization of (4.5) we use the Euler–Maruyama method; i.e., the discrete scheme is

$$w_{t_{k+1}} = w_{t_k} - \Delta t\, w_{t_k-\tau} + \sigma\sqrt{\Delta t}\,\mathcal{N}_{0,1}, \qquad k = 1, 2, \ldots, K, \tag{4.6}$$

subject to the initial condition wt ≡ 1 for t ≤ 0. Here K = T /Δt denotes the total number of timesteps, tk = kΔt, and N0,1 a normally distributed random variable with zero mean and unit variance. Note that the values of τ are chosen to be integer multiples of Δt, so that tk − τ = tl for some l □ Z. For each (σ, τ)-pair and each path q of the Monte Carlo simulation we calculate the "indicator,"

$$I_{\sigma,\tau} := \frac{1}{Q}\sum_{q=1}^{Q}\left(\Delta t \sum_{k=(T-1)/\Delta t}^{T/\Delta t} |w_{t_k}^q|^2\right)^{1/2},$$

where wq t is the qth path in the Monte Carlo simulation of (4.6). The shading in Figure 2 encodes the logarithm of Iσ,τ . To define a region of "numerical convergence," we choose a threshold Θ such that I0,τc = Θ for the delay τc = π 2 that is critical for the problem without noise (σ = 0). In our case this led to Θ∼-10−2. The region of "numerical convergence" is marked dark blue in Figure 2. We observe the decrease of the critical value of the delay with increasing level of noise. For comparison, the critical values of τ given by (3.20) as a function of σ are indicated by the solid line.

4.4. **Numerical study of system (2.2) with fixed communication matrix**. We present results of numerical simulations of system (2.2) in the one-dimensional setting d = 1, where we fix the communication rates to ψij ≡ 1 for all i, j = 1, 2,...,N; i.e., every agent communicates with all others at the same rate. Consequently, the communication matrix A has the off-diagonal entries Aij = −1, i = j, and Aii = N −1. It has only two eigenvalues, 0 and N. Consequently, its Fiedler number is μ2 = N,

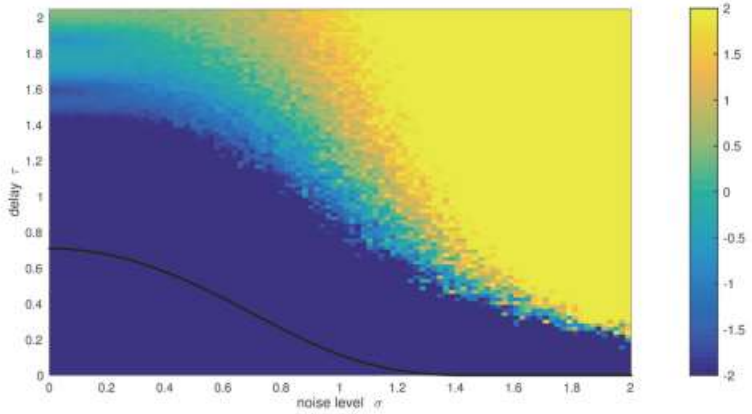

Fig. 2. Results of Monte Carlo simulations of the delayed SDE (4.5) with Q = 100 paths for (σ, τ) □ [0, 2] × [0, 2]. The shading encodes log(Iσ,τ). The region of "numerical

convergence" is dark blue. The solid line indicates the critical values of τ given by formula (3.20) with λ = 1 as a function of σ.

and we can choose := N in (3.2). In this setting, we can directly compare our analytical result, Theorem 3.1, with numerical simulations. We will be considering even numbers of agents N = 2K, particularly, N □ {2, 20}, and we prescribe the initial datum

$$v_i(t) \equiv \begin{cases} -1 & \text{for } i = 1, 2, \dots, K, \\ 1 & \text{for } i = K+1, K+2, \dots, N \end{cases} \tag{4.7}$$

for t □ (−τ, 0]. Although the asymptotic behavior of the solutions in general depends on the particular choice of the initial datum, a systematic study of this dependence is beyond the scope of this paper. Therefore we consider only the "generic" choice of initial conditions (4.7).

We perform Monte Carlo simulations of the system (2.2) with N □ {2, 20}, σi = σ for all i = 1, 2,...,N, and λ = 1 (other values of λ can be achieved by rescaling of σ and time). We divide the domain [0, 2]×[0, 2] for (σ, τ) into 50×50 equidistant (σ, τ)- pairs. For each pair of the parameter values we perform a Monte Carlo simulation with Q = 100 paths over the time interval [0, T] with T = 30. We use the Euler– Maruyama method for discretization of (2.2) with timestep Δt = 10−3. To classify the asymptotic behavior of the solution, we again define the "indicator"

$$I_{\sigma,\tau} := \frac{1}{Q} \sum_{q=1}^{Q} \left(\frac{\Delta t}{N} \sum_{k=(T-1)/\Delta t}^{T/\Delta t} |\mathbf{v}_{t_k}^q|^2 \right)^{1/2}, \tag{4.8}$$

where vq tk is the qth path in the Monte Carlo simulation of (1.1)–(1.2) at time tk = kΔt. We say that numerical flocking takes place when Iσ,τ < 10−2. The shading in Figure 3 encodes the decadic logarithm of the indicator, and the dark blue region indicates numerical flocking. We observe that the region of numerical flocking is only weakly influenced by the number of agents N. This is in agreement with the fact that the flocking condition (3.6) in Theorem 3.1 does not depend on N. The increased smoothness of the color transition when N = 20 is a consequence of the law of large

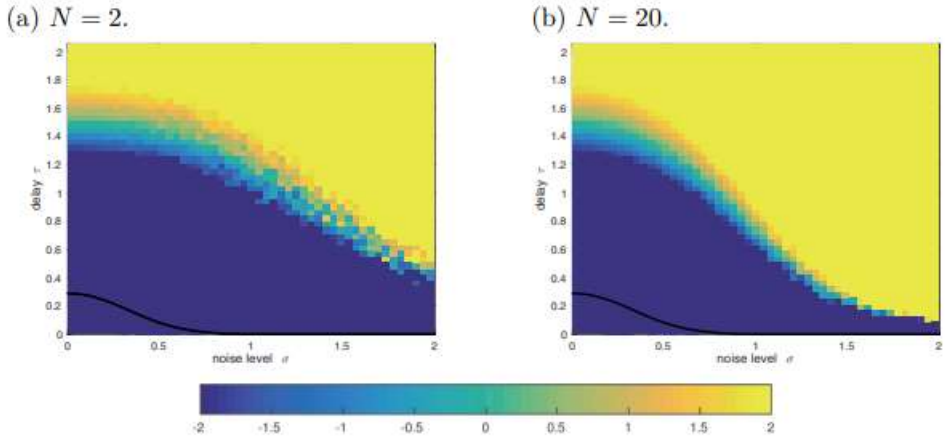

Fig. 3. Decadic logarithm of the indicator $I_{\sigma,\tau}$, given by (4.8), for Monte Carlo simulations of the system (2.2) with Q = 100 paths on the time interval [0, 30] subject to the initial condition (4.7), with $\lambda = 1$, $(\sigma, \tau) \in [0, 2] \times [0, 2]$. The dark blue regions (color online) indicate "numerical flocking." The solid line indicates the critical value τ_c given by (3.6) for $\lambda = 1$ as a function of σ. The number of individuals is (a) N = 2 and (b) N = 20.

numbers. For comparison, the critical value τ_c given by (3.6) for $\lambda = 1$ as a function of σ is indicated by the solid line in both panels. The comparison with the numerical results suggests that the condition (3.6) is far from optimal.

4.5. **Numerical study of the delayed Cucker–Smale system with multiplicative noise.** Finally, we present results of numerical simulations of system (1.1)–(1.2) with communication rates $\psi(|x_i - x_j|)$ and ψ given by (1.3). As in section 4.3, our goal is to characterize the asymptotic behavior of the solutions in dependence on the parameter values; however, we are facing additional difficulties here. In particular, the asymptotic behavior of the solution may depend nontrivially on the initial condition, as we show in Figure 4. Since a systematic study taking this effect into account is beyond the scope of this paper, we will impose the same type of initial condition for all our simulations. In particular, we prescribe constant zero value for the x-variables,

$$x_i(t) \equiv 0 \qquad \text{for } t \in (-\tau, 0],\ i = 1, 2, \ldots, N. \tag{4.9}$$

For the v-variables we impose again the initial datum (4.7).

We perform Monte Carlo simulations of the system (1.1)–(1.2), (1.3) with $N \in \{2, 20\}$ and $\beta = 0.1$ (strong coupling) or $\beta = 1$ (weak coupling). As in section 4.3, we fix $\lambda = 1$ and divide the domain $[0, 2] \times [0, 2]$ for (σ, τ) into 50×50 equidistant (σ, τ)- pairs. For each pair of the parameter values we perform a Monte Carlo simulation with Q = 100 paths over the time interval [0, T] with T = 30. We use the Euler– Maruyama method for discretization of (1.1)–(1.2) with timestep $\Delta t = 10^{-3}$. To classify the asymptotic behavior of the solution, we again use the indicator (4.8) and say that numerical flocking takes place when $I_{\sigma,\tau} < 10^{-2}$. The background color in Figure 5 encodes the decadic logarithm of the indicator, and the dark blue region indicates numerical flocking.

In panel (a) we indicate by an arrow the point $(\sigma, \tau) = (0, 1.75)$ that corresponds to the parameter setting in Figure 4; however, note that the initial conditions for xi in Figure 4 differ from (4.9). We see that the indicated point lies close to the

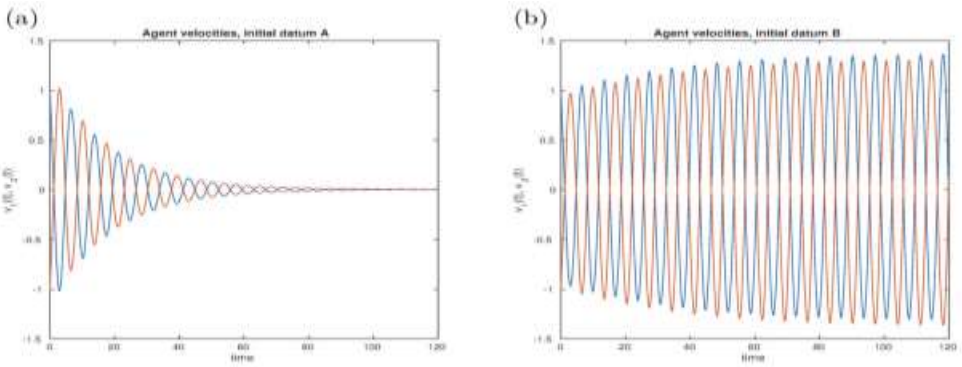

Fig. 4. Numerical simulations of the system (1.1)–(1.2), (1.3) with parameter values N = 2, λ = 1, β = 0.1, σ = 0, and τ = 1.75. Both simulations are performed on the time interval [0, 120] with discrete timestep Δt = 10−3. The initial condition for v is v1(t) ≡ 1, v2(t) ≡ −1 for t □ (−τ, 0] in both cases. The initial condition for x is (a) x1(t) ≡ −1, x2(t) ≡ 1; (b) x1(t) ≡ 1, x2(t) ≡ −1. The plots show the velocities of the two agents (red and blue, color online) as functions of time.

boundary of the dark blue region, i.e., in the "transition zone" between numerical flocking and nonflocking. We hypothesize that this is why we were able to observe the two qualitatively different kinds of asymptotic behavior in Figure 4 even if the initial datum for the v-variables is the same in both cases. Again, a systematic study of this hypothesis is beyond the scope of this paper.

In Figure 5 we observe that the region of numerical flocking is only weakly influenced by the number of agents N. This is in agreement with the fact that the flocking condition (3.6) in Theorem 3.1 does not depend on N. The increased smoothness of the color transition when N = 20 is a consequence of the law of large numbers. On the other hand, we can distinguish two distinct types of patterns, one similar to Figure 2 for the strong coupling case β = 0.1 (Figures 5(a) and 5(b)), and a semicircular pattern for the weak coupling case β = 1 (Figures 5(c) and 5(d)). In particular, the result for the weak coupling case is somewhat surprising—it suggests that for low levels of noise (σ 0.6), introduction of intermediate delays (0.3 τ 1.8) may facilitate flocking. This is further supported by Figure 6 where we plot sample solutions of (1.1)–(1.2), (1.3) for N = 2, β = 1, σ = 0 (Figure 6(a)), σ = 0.5 (Figure 6(b)) and three different values of the delay τ □ {0, 1, 2}. We observe that while for τ = 0 and τ = 2 the agents do not show the tendency to converge to a common velocity during the indicated time interval, they exhibit numerical flocking for the intermediate value τ = 1. We will call this observation time-delay–induced flocking.

Let us note that the results presented in Figure 6 do not contradict our analytical results. In particular, condition (3.6) gives τ < √2/4 . = 0.35 if σ = 0 and τ < (−1/2 + -11/8)/4 . = 0.17 if σ = 0.5, so it is only satisfied for the simulations in the panels corresponding to τ = 0 in Figure 6. Therefore, the statement of Lemma 3.4 applies. The (expectation of) the Lyapunov function (3.13) decreases in time for these two simulations.

To gain a further understanding of the interesting phenomenon of time-delay– induced flocking, we run systematic simulations of the system (1.1)–(1.2), (1.3) with

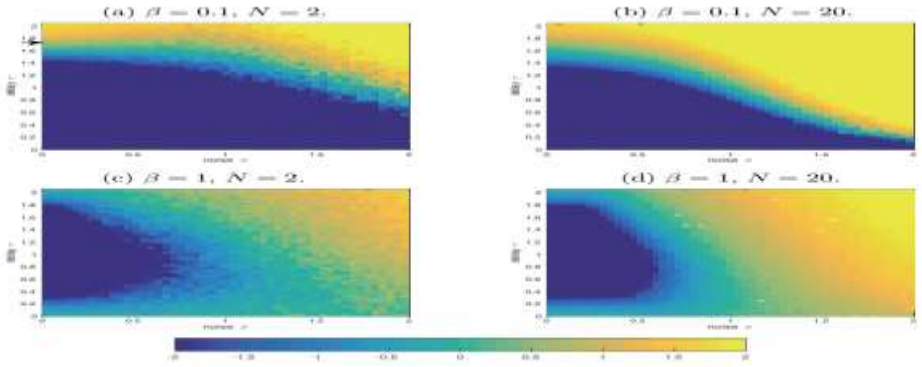

Fig. 5. Decadic logarithm of the indicator Iσ,τ , given by (4.8), for Monte Carlo simulations of the system (1.1)–(1.2), (1.3) with Q = 100 paths on the time interval [0, 30] subject to the initial conditions (4.7) and (4.9), with λ = 1 and (σ, τ) □ [0, 2] ×[0, 2]. The dark blue regions (color online) indicate numerical flocking. The arrow in (a) indicates the point (σ, τ) = (0,

1.75) that corresponds to the parameter setting in Figure 4. We use (a) β = 0.1, N = 2; (b) β = 0.1, N = 20; (c) β = 1, N = 2; and (d) β = 1, N = 20.

different values of β □ [0.5, 2.5], τ □ [0, 2], and σ □ {0, 0.5}. We calculate the indicator Iβ,τ as in (4.8) with Q = 1 for σ = 0 (there is no need to run more than one path for the case without noise) and Q = 100 Monte Carlo paths for σ = 0.5. The decadic logarithm of Iβ,τ is plotted in Figure 7, and we again use the threshold Iβ,τ < 10−2 to define numerical flocking (dark blue regions in Figure 7). We observe that there exists (for β sufficiently large) a region of intermediate values of τ where numerical flocking takes place, while there is no flocking for smaller or larger τ values. Moreover, we see that noise has a disruptive influence on flocking (the dark blue region is smaller in Figure 7(b) compared to Figure 7(a)).

5. Discussion. We have studied a generalization of the Cucker–Smale model accounting for measurement errors, through introduction of multiplicative white noise, and for delays in information processing. This has led to a system of stochastic delayed differential equations, (1.1)–(1.2). In section 3, we have considered the communication rates between agents as given stochastic processes and derived a sufficient condition for flocking, which we define as asymptotic convergence of the agents' velocities towards a common value. The condition is given in terms of the critical delay that guarantees

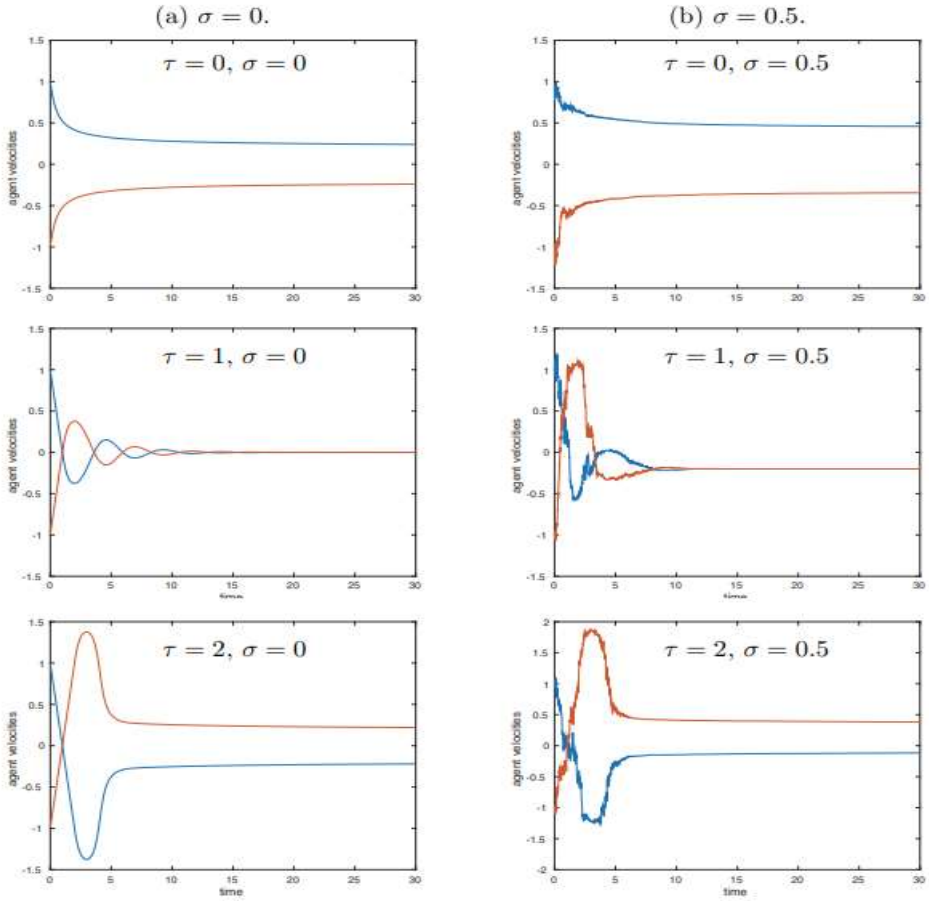

Fig. 6. Agent velocities v1(t), v2(t) in sample solutions of the system (1.1)–(1.2), (1.3) with N = 2, λ = 1, β = 1 (weak coupling), on the time interval [0, 30] subject to the initial conditions (4.7) and (4.9). We use (a) σ = 0 and (b) σ = 0.5.

ISSN PRINT 2319 1775 Online 2320 7876
 UGC CARE Listed (Group -I) Journal Volume 11, Iss 01, 2022

flocking as a function of the noise level. Our analysis is based on the construction of a suitable Lyapunov function for the system and a study of its decay. As a by-product of the analysis, we obtained a sufficient condition for asymptotic convergence of delayed geometric Brownian motion.

The second part of the paper was devoted to systematic numerical simulations. First, we performed Monte Carlo simulations of delayed geometric Brownian motion and evaluated its asymptotic behavior based on a suitable "numerical indicator." This led to the conclusion that the analytically derived sufficient condition for asymptotic convergence is qualitatively right—the convergence deteriorates with increasing noise level and delay. However, quantitatively this condition is far from optimal. Next, we simulated the Cucker–Smale-type system with fixed communication rates and again compared the outcome with the analytical result. As before, the comparison showed

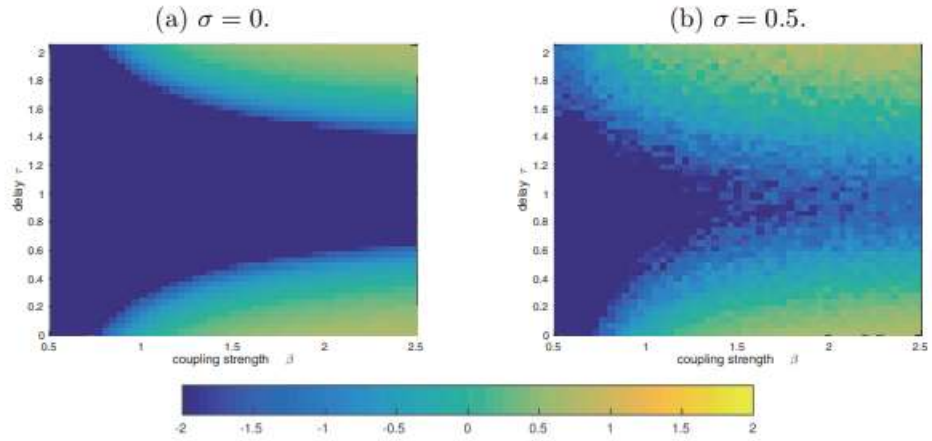

Fig. 7. Decadic logarithm of the indicator Iβ,τ for simulations of the system (1.1)–(1.2), (1.3) on the time interval [0, 30] with λ = 1, N = 2, (β, τ) □ [0.5, 2.5] × [0, 2]. We use (a) σ = 0, Q = 1 and (b) σ = 0.5, Q = 100. The dark blue regions (color online) indicate numerical flocking.

that, while qualitatively correct, the analytical formula produces too restrictive critical delays. Finally, we simulated the full Cucker–Smale system with delays and multiplicative noise. We used two regimes for the dependence of the communication rates on the agents' distances: the strong coupling regime, which leads to unconditional flocking in the "classical" Cucker–Smale model, and the weak coupling regime, where flocking may or may not take place. In the strong coupling regime the numerical picture was similar to the previous simulation with fixed communication rates. On the other hand, in the weak coupling regime we observed a somewhat surprising behavior of the system—namely, that the introduction of an intermediate time delay may facilitate flocking. We call this phenomenon "time-delay–induced flocking."

Our paper leaves several open questions. First of all, our analytical flocking condition is too restrictive compared to numerical results, so efforts should be made to improve it. Moreover, the analysis applied to the case when the communication rates are given and satisfying a certain structural assumption. This is in fact against the spirit of the original Cucker–Smale model where the communication rates depend on the mutual distances between agents. A possible extension of our analysis to this case remains an open problem. The main difficulty

is due to the fact that it is not clear how to apply the classical bootstrapping argument that bounds the velocity fluctuations in terms of fluctuations in positions and vice versa. For the numerical part, it would be desirable to apply some multilevel Monte Carlo or importance sampling technique to obtain more accurate results. Moreover, the influence of the initial condition on the asymptotic behavior should be studied. Finally, the interesting phenomenon of delayinduced flocking deserves a detailed study, from both the analytical and numerical points of view.

Acknowledgment. The work on this paper was partially completed during the program "Stochastic Dynamical Systems in Biology: Numerical Methods and Applications," which the authors would like to thank the Isaac Newton Institute for Mathematical Sciences, Cambridge, for supporting and being hospitable to them during.

REFERENCES

[1] S. Ahn and S.-Y. Ha, Stochastic flocking dynamics of the Cucker–Smale model with multiplicative white noises, J. Math. Phys., 51 (2010), 103301, doi:10.1063/1.3496895.

[2] J. Appleby, X. Mao, and M. Riedle, Geometric Brownian motion with delay: Mean square characterisation, Proc. Amer. Math. Soc., 137 (2009), pp. 339–348, doi:10.1090/ S0002-9939-08-09490-2.

[3] J. A. Carrillo, M. Fornasier, J. Rosado, and G. Toscani, Asymptotic flocking dynamics for the kinetic Cucker–Smale model, SIAM J. Math. Anal., 42 (2010), pp. 218–236, doi: 10.1137/090757290.

[4] J. Carrillo, M. Fornasier, G. Toscani, and F. Vecil, Particle, kinetic, and hydrodynamic models of swarming, in Mathematical Modeling of Collective Behaviour in Socio-Economic and Life Sciences, Model. Simul. Sci. Tech., G. Naldi, L. Pareschi, and G. Toscani, eds., Birkh¨auser, Cambridge, MA, 2010, pp. 297–336, doi:10.1007/978-0-8176-4946-3 12.

[5] F. Cucker and S. Smale, Emergent behaviour in flocks, IEEE Trans. Automat. Control, 52 (2007), pp 852–862, doi:10.1109/TAC.2007.895842.

[6] F. Cucker and S. Smale, On the mathematics of emergence, Japan. J. Math., 2 (2007), pp. 197–227, doi:10.1007/s11537-007-0647-x.

[7] L. El'sgol'ts and S. Norkin, Introduction to the Theory and Application of Differential Equations with Deviating Arguments, Academic Press, New York, 1973 (translated by J. Casti).

[8] R. Erban, From molecular dynamics to Brownian dynamics, Proc. Roy. Soc. A, 470 (2014), 20140036.

[9] R. Erban, Coupling all-atom molecular dynamics simulations of ions in water with Brownian dynamics, Proc. Roy. Soc. A, 472 (2016), 20150556, doi:10.1098/rspa.2015.0556.

[10] R. Erban and J. Haskovec, From individual to collective behaviour of coupled velocity jump processes: A locust example, Kinetic Rel. Models, 5 (2012), pp. 817–842, doi:10.3934/ krm.2012.5.817.

ISSN PRINT 2319 1775 Online 2320 7876
 UGC CARE Listed (Group -I) Journal Volume 11, Iss 01, 2022

[11] S. Gillouzic, Fokker-Planck Approach to Stochastic Delay Differential Equations, Doctoral Thesis, Ottawa-Carletan Institute for Physics, University of Ottawa, Ottawa, Canada, 2000.

[12] S.-Y. Ha, K. Lee, and D. Levy, Emergence of time-asymptotic flocking in a stochastic CuckerSmale system, Comm. Math. Sci., 7 (2009), pp. 453–469, doi:10.4310/cms.2009.v7.n2.a9.

[13] S.-Y. Ha and J.-G. Liu, A simple proof of the Cucker-Smale flocking dynamics and mean-field limit, Comm. Math. Sci., 7 (2009), pp. 297–325, doi:10.4310/cms.2009.v7.n2.a2.

[14] S.-Y. Ha and E. Tadmor, From particle to kinetic and hydrodynamic descriptions of flocking, Kinetic Rel. Models, 1 (2008), pp. 315–335, doi:10.3934/krm.2008.1.415.

[15] J. Haskovec, Flocking dynamics and mean-field limit in the Cucker-Smale-type model with topological interactions, Phys. D, 261 (2013), pp. 42–51, doi:10.1016/j.physd.2013.06.006.

[16] D. Hunt, G. Korniss, and B. Szymanski, Network synchronization in a noisy environment with time delays: Fundamental limits and trade-offs, Phys. Rev. Lett., 105 (2010), 068701, doi:10.1103/physrevlett.105.068701.